Biointerface Research in Applied Chemistry
Open-Access Journal (ISSN: 2069-5837)

Article
Volume 14, Issue 2, 2024, 29
https://doi.org/10.33263/BRIAC142.029

Mesoporous CA/PEG Membrane-Modified TiO_2 Nanoparticles with Improved Desalination Performance

Faizal Mustapa [1, 2], Muhammad Nurdin [3,*], Muh. Zakir Muzakkar [4], Muhammad Idris [5]

[1] Doctoral student of Agricultural Sciences, Universitas Halu Oleo, Kendari 93121 – Southeast Sulawesi, Indonesia
[2] Department of Marine Sciences, Institut Teknologi dan Bisnis Muhammadiyah Kolaka, Kolaka 93511 – Southeast Sulawesi, Indonesia
[3] Department of Chemistry, Faculty of Mathematics and Natural Sciences, Universitas Halu Oleo, Kendari 93231 – Southeast Sulawesi, Indonesia
[4] Department of Chemistry, Faculty of Mathematics and Natural Sciences, Universitas Halu Oleo, Kendari 93231 – Southeast Sulawesi, Indonesia
[5] Department of Agriculture Sciences, Universitas Halu Oleo, Kendari 93231 – Southeast Sulawesi, Indonesia
* Correspondence: mnurdin06@yahoo.com; (M.N.)

Scopus Author ID 56678695400
Received: 24.02.2023; Accepted: 23.02.2023; Published: 3.02.2024

Abstract: Water is one of the abiotic components that play an important role in the continuity and improvement of the quality of human life. In addition, water also needs to improve its quality so that it is safe for human consumption. In this case, we utilize seawater to be processed into usable water for clean water purposes for humans by designing a reverse osmosis method using cellulose acetate (CA), polyethylene glycol (PEG) combined with TiO_2 nanoparticles (TiO_2-NPs) in an effort to desalinate seawater. Firstly, the fabrication of CA/PEG/TiO_2 membrane by comparing the effectiveness methods over surface coating (*SC*) and blending (*B*), which is proven by chemical-physical data (crystallinity, functional groups, and morphology), and secondly, membrane performance tests (water flux, salt rejection, pH, and salt content). Refers from the results showed that the fabrication of CA/PEG/TiO_2 membrane by *B* method has good performance in desalinating seawater as evidenced by semi-crystalline form with good porosity in filtering seawater with water flux value of 161.18 L/m^2.h and salt rejection of 84% that indicated the 4‰ for water salinity. The acidic condition also showed that the *SC* and *B* methods exhibit stability acidic with a pH value of 7.8. The seawater desalination RO system provides a good ability to reduce salt content in seawater. This study is evidenced to contribute to the innovation of seawater processing into clean water for further utilization against coastal communities and small islands in Indonesia.

Keywords: Membrane; TiO_2; Reverse Osmosis; Desalination; Seawater

1. Introduction

Water is the most important basic human need for human survival and quality of life, but not all areas have good water resources. Coastal areas and small islands have very poor clean water sources, so problems arise in fulfilling the need for clean water for daily needs [1]. In Indonesia, the threat of lack of clean water increases every year. Indonesia can actually utilize the abundant amount of seawater as an alternative raw material to fulfill the community's need for clean water. As mentioned above, the largest water supply in Indonesia is seawater [2]. The problem is that seawater has a lot of excess mineral content, bacteria, and impurities, such as small solids, so it cannot be consumed by humans directly [3].

The freshwater resources owned by each country in the world show that Indonesia is ranked 51st with a high level of crisis risk (High 40-80% possibility) [4]. The main problem faced in relation to water resources is the quantity of water that can no longer meet the increasing demand and the quality of water for domestic use, which is decreasing from year to year [5]. The percentage of water found on Earth is 97%, but water that is suitable for consumption is only around 27%. In short, water availability on Earth is very large, but the amount that can be used is very small [6]. Water is a natural material needed for human, animal, and plant life, namely as a medium for transporting food substances, as well as a source of energy and various other purposes [7]. Seawater's potential is interesting to explore because Indonesia is a maritime country with 75% water area. Unfortunately, seawater has a lot of excess mineral content, bacteria, and impurities that humans cannot use directly. To overcome these problems, it is necessary to protect existing water resources through appropriate water treatment strategies.

Membrane technology is an effective approach to seawater treatment. The advantages of using membranes are simple operation, cost-effective, no phase change, high productivity, easy scaling, and high purification [8]. Many types of membranes have been applied in water treatment, such as microfiltration (MF), ultra-filtration (UF), nanofiltration (NF), and Reverse Osmosis (RO). RO is seen as a good and efficient membrane today, as it is denser and is a high-pressure-driven filtration process with a narrow pore size range (<0.001 μm), thus almost separating all ions [9]. A membrane is a thin layer between two fluid phases, namely the feed phase and the permeate phase. It acts as a barrier to a certain species, which can separate substances of different sizes and limit the transport of various species based on their physical and chemical properties [10]. Membrane technology has a major influence on the purification process of seawater and wastewater. The need for clean water and the scarcity of water sources are major driving factors in developing membrane technology [11]. Membrane-based technology is the main tool for seawater treatment and desalination. At this point, highly selective membrane technologies, such as reverse osmosis (RO), membrane distillation (MD), and Pervaporation (PV), have become the most explored membranes in the field of seawater desalination [12].

Several nanoparticles, such as zeolite, carbon nanotubes, silica, clay, and graphene oxide, have been used to modify RO membranes [13]. All modified membranes showed a high salt content reduction; however, RO membranes still have significant disadvantages due to the occurrence of membrane fouling, such as water flux declination, resulting in increased operating costs and reduced membrane lifetime. Integrating photocatalytic oxidation and membrane filtration is a good approach to reducing fouling adsorption on the membrane surface. The utilization of titanium dioxide nanoparticles (TiO_2-NPs) as a photocatalytic material has attracted attention among industries due to its good photocatalytic properties, distinct electronic properties, high material surface effectiveness, and ability to destroy organic contaminants in wastewater [14].

Besides its photocatalytic properties, TiO_2-NP_s have also been reported as water disinfection and antifouling [15]. In addition, RO membranes using Cellulose Acetate (CA) material and the addition of Polyethylene Glycol (PEG) additives have found good results in seawater salt rejection [16]. However, using CA is susceptible to microbial attack, which can cause fouling on the membrane surface [17]. An effective strategy to overcome this limitation is modifying the sublayer using functional nanomaterials to mediate the adsorption rate. The innate properties of functional nanomaterials, such as hydrophilicity, antifouling, interactive

affinity, photocatalytic, and others, can complement the weaknesses of the membrane to obtain the desired properties by adding PEG-modified TiO_2-NPs.

The approach of membrane modification with TiO_2 has increased membrane flux. Based on Al Mayyahi's report, the membrane permeability increased with the addition of TiO_2-NPs, and the modified membrane showed good fouling resistance under ultraviolet (UV) light. Damodar *et al*. also reported that the modification of TiO_2-NPs into polyvinylidene fluoride (PVDF) membrane exhibited excellent self-cleaning, antibacterial, and photocatalytic properties; however, UV irradiation markedly increased the operating cost, hindering the practical application of TiO_2-NPs based on the antifouling membrane.

Additives are often added to membranes for specific purposes, like highly properties materials to improve membrane performance. In addition, the number of additives can affect the number and pore size of the resulting membrane. The type of additive usually used is PEG, which is one of the substances that can be used to form and control pore size and structure [18,19]. Adding PEG to the membrane can produce smaller, more regular pore membranes, increasing the flux value [20]. So in this work, we explore the desalination process using CA/PEG/TiO_2 membrane by optimization preparation over SC and B methods in order to desalination performance against seawater from Kolaka Beach, Kolaka Regency, Southeast Sulawesi Province, Indonesia, where many people around Kolaka Beach still have difficulty fulfilling their daily clean water needs.

2. Materials and Methods

2.1. Preparation of seawater.

Seawater samples were taken from Kolaka Beach, located in Kolaka Regency, Southeast Sulawesi Province, and put into a 19-liter gallon. Then, it was filtered using a filter cloth to separate impurities included when taking seawater samples. The filtered filtrate was put back into a clean gallon for desalination testing using a modified membrane.

2.2. Preparation of CA/PEG membrane.

CA/PEG membrane preparation as a control was carried out based on the procedure performed. Briefly, 3 grams of CA was dissolved in 17 mL of acetone and stirred using a magnetic stirrer; then, 2 grams of PEG was added and stirred for approximately 3 hours at room temperature. Then, the CA/PEG membrane was printed on a Petri dish and allowed to stand to remove bubbles for 15 hours. The membrane was slowly released from the Petri dish mold, and the CA/PEG membrane was obtained.

2.3. Preparation of CA/PEG membrane-modified TiO_2-NPs.

The fabrication of TiO_2-NPs modified CA/PEG membrane was conducted by 2 (two) methods referred to Ounifi *et al*. (2022), namely the methods of (i) surface coating (*SC*) and (ii) blending (*B*). Firstly, the *SC* method to fabricate the CA/PEG/TiO_2 membrane was applied by preparing a precursor of 0.5 grams of TiO_2 and printing by sprinkling it on the surface of CA/PEG membrane. Secondly, the mixing method was made by stirring with the addition of 0.5 grams of TiO2 mixed with the CA/PEG membrane. After homogeneity, the CA/PEG/TiO_2 membrane solution was printed on a petri dish and allowed to stand for 15 hours until a dry membrane was obtained.

2.4. Characterization of membranes.

Membrane characterization was conducted using X-ray diffraction (XRD) to determine the deposition of TiO_2-NPs on the CA/PEG membrane and the crystallinity of CA/PEG/TiO_2 membranes. Fourier transforms infrared (FTIR) was applied to determine the functional groups contained in the membrane and identify the CA/PEG membrane. In addition, scanning electron microscope (SEM) identification was also used to observe the membrane's morphological structure, cross-section, and thickness. Through this analysis, the condition of membrane porosity and the presence of TiO_2 on the surface of the membrane with a specific characteristic can be seen.

2.5. Reverse osmosis test.

The design of an RO system was examined from a polyvinyl chloride (PVC) pipe with a diameter of 2 inches with three processing tubes. Wherein the first tube contains feed water (sample). The second tube has an initial pretreatment consisting of sand, charcoal, gravel, and fiber. In the last tube, a membrane has been fabricated and placed horizontally, designed with UV light for high-performance TiO_2-NPs material on the CA/PEG membrane. The design of the RO filtration device can be seen in Figure 7. The seawater desalination testing process applied 19 liters of seawater, put it in a charcoal bucket, and soaked it for 24 hours.

Furthermore, the water is filtered and put into tube one, the feed water container. Then, water was forwarded to a tube containing sand, charcoal, gravel, and palm fiber filter materials. Finally, the test water enters tube 3 of the filtration process using a membrane illuminated by UV light.

2.6. Membrane performance test.

Water flux shows the ability of water to pass through the membrane. The results of the desalination test obtained permeate in units of time, the membrane area used, and the time used for testing. To calculate the water flux, can apply with the equation below [22]:

$$J = \frac{Q}{(A \times t)} \quad (1)$$

Where, J is flux volume (L/m^2.h), A is membrane surface area (m^2), t is time duration (hour), and Q is permeating volume (L). In addition, the salt rejection was also identified to measure the salt content separated from the feed water carried by the rejection water. The salt rejection can be determined by using the equation below [22]:

$$R = \left(1 - \frac{C_p}{C_0}\right) \times 100\% \quad (2)$$

Where, R is salt rejection (%), Cp is the salination concentration of permeate (‰), and C0 is the salination concentration of the sample (initial sample) (‰). Furthermore, the acidity (pH) was determined to identify the sum of hydrogen ion (H^+) concentrations in a solution that expresses its acidity and validity in salt water. Finally, salt content was determined using a salinity meter to observe the dissolved salt content in seawater. The higher salinity value is proportional to the higher chemical contents such as chloride, bromide, and iodide in the seawater. The diagram of the membrane preparation procedure is shown in the following Figure 1.

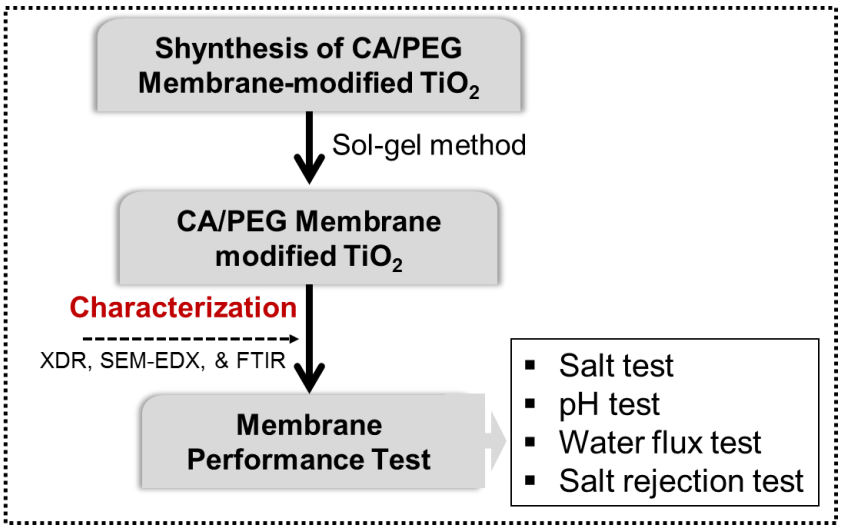

Figure 1. The diagram of the membrane preparation procedure.

3. Results and Discussion

3.1. Preparation of CA/PEG Membrane Modified with TiO_2-NPs.

Nanotechnology is one of the promising materials considering its excellent strength and excellent performance effectiveness in various aspects such as energy, biotechnology, sensors, and membranes [23,24]. In line with the development of nanotechnology in the field of membranes, it becomes an interesting issue in approaching an effective water filtration process by looking at the aspect of optimizing the retained or retained material to be filtered so that previously turbid water becomes clear or good quality [25,26]. This research examined nanotechnology based on nanoparticles categorized into several categories, such as membrane manufacturing as crystallinity data identified by XRD, chemical elements using FTIR, and physics with SEM instrumentation. The instrumentations above represent the characteristics of successfully fabricating the CA/PEG/TiO_2 membrane.

Based on Figure 2 can be seen the fabricated membrane based on cellulose acetate (CA) and polyethylene glycol (PEG) with the same ratio to observe the distribution and durability of a suitable membrane between *SC* and *B* methods when adding TiO_2-NPs. Physically, it can be seen that CA/PEG (Figure 2a) is a control (CA/PEG) before adding TiO_2-NPs, which gives a slightly transparent color compared to those added with TiO_2-NPs.

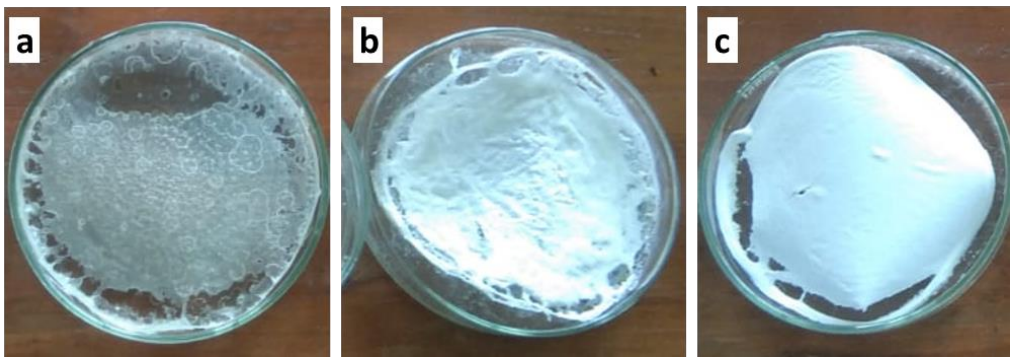

Figure 2. Fabrication of membranes; **(a)** CA/PEG, **(b)** CA/PEG/TiO_2 *SC*, and **(c)** CA/PEG/TiO_2 *B*.

Figure 2b shows that the membrane fabricating process by the *SC* method has the characteristics of a slightly rough membrane surface due to the TiO_2-NPs attachment technique that occurs on the membrane surface randomly (uneven). In addition, the preparation of the

membrane by *B* method (Figure 2c) provides a slightly smooth membrane surface because the distribution of TiO_2-NPs is evenly distributed in the membrane grid, so it can be ascertained that the membrane with the B method for the process of adding TiO_2-NPs provides an excellent visual membrane.

3.2. Characterisation of CA/PEG Membrane modified with TiO_2-NPs.

3.2.1. X-ray diffraction (XRD).

The results of membrane crystallinity analysis using the XRD instrument (Figure 3) showed differences in each membrane's peak intensity. The sharp intensity characterizes the membrane as semi-crystalline. Membranes with a semi-crystalline model have a good impact on membrane durability because it also significantly affects membrane durability in addition to a slightly elastic membrane.

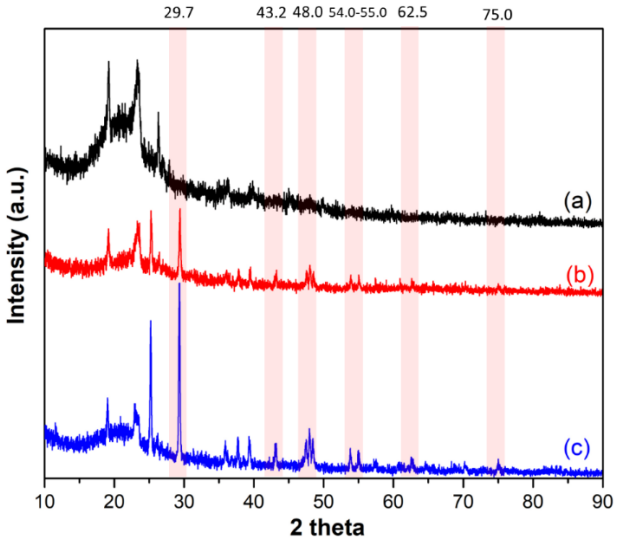

Figure 3. XRD patterns of the fabricated membranes, **(a)** CA/PEG, **(b)** CA/PEG/TiO_2 *SC*, and **(c)** CA/PEG/TiO_2 *B*.

Figure 3 shows that without adding TiO2-NPs (Figure 3a), the intensity at 2 theta 29.7° characterizes the miller index 311 with the H-titanate model with confirmed $H_2Ti_5O_{11}.H_2O$ [27]. This condition occurs because the organic materials of CA and PEG form polymers and have been inserted by sol-gel TiO_2-NPs in the membrane matrix that is likely to interact between materials [28]. In addition, the anatase TiO_2 crystals were identified at 2 theta of 25° (1 0 1), 48.0° (2 0 0), 54.0 (1 0 5), 55.0 (2 1 1), 62.5° (2 0 4), 75° (2 1 5) and a few rutile TiO_2 crystals formed at 43.2° (2 1 0) [29]. Evidence suggests that the CA/PEG matrix and TiO_2-NPs interaction is a Van Der Waals bond where hydrogen bonds are formed between hydroxyl groups in CA and form a network between OH groups [30].

3.2.2. Fourier Transform Infra-Red (FTIR).

FTIR is used to identify the functional groups of the membrane that have been identified. Based on the FTIR spectra (Figure 4), it has been characterized from wavenumbers (cm^{-1}) 350 cm-1 to 4000 cm^{-1}. The analysis results show that several functional groups are identified based on the absorption of certain wave numbers of each modified membrane.

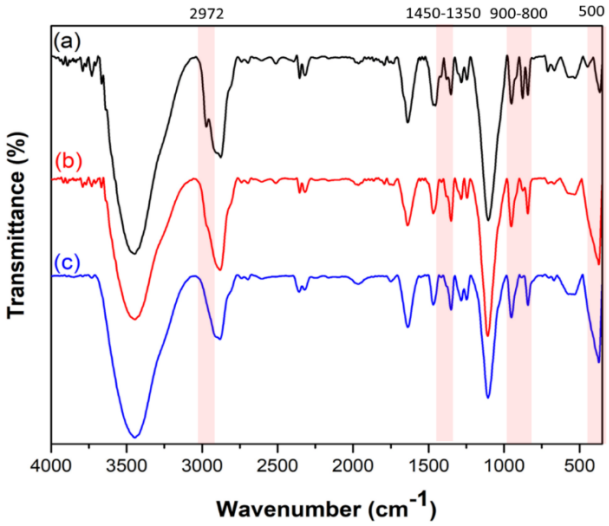

Figure 4. FTIR spectra of the fabricated membranes, **(a)** CA/PEG, **(b)** CA/PEG/TiO_2 *SC*, and **(c)** CA/PEG/TiO_2 *B*.

Table 1. Results of FTIR data interpretation.

Wavenumbers (cm^{-1})	**Functional Groups**	**CA/PEG**	**CA/PEG/TiO_2 *SC***	**CA/PEG/TiO_2 *B***
		(a)	**(b)**	**(c)**
3444.87	-OH	√	√	√
2972.31	Alkane (C-H) (strong)	√	√	-
2879.72	Alkane (C-H) (strong)	√	√	√
2353.16	Alkane (C-H) (strong)	√	√	√
1639.49	Alkene (C=H)	√	√	√
1467.83	Alkane (C-H) (strong)	√	√	√
1381.03	Aliphatic Alkanes (C-H)	√	√	-
1284.59	Alkane (C-H) (strong)	√	√	√
1244.09	C-O-C stretching	√	√	√
1109.07	Alcohol, ether, carboxylic acid (C-O)	√	√	√
952.84	Alkene (C=H) (strong)	√	√	√
875.68	Cyclo-pyranose (CA)	√	√	-
842.89	Aromatic (C-H)	√	√	√
372.26	O-Ti-O	-	√	√

CA/PEG control membrane, CA/PEG/TiO_2 *SC* and *B* methods have identified several functional groups formed at wave number 3444 cm^{-1}. There is an -OH group derived from CA and PEG, wavenumbers 2879 cm^{-1}, 2353 cm^{-1}, 1467.83 cm^{-1}, and 1284 cm^{-1} identified C-H alkane bonds, wave numbers 1639 cm^{-1} and 952 cm^{-1} indicate the presence of an alkene group (C=H), and 842 cm^{-1} has the same aromatic group (C-H). Uniquely, the CA/PEG/TiO_2 membrane with the *B* method does not show aliphatic alkane functional groups 1381 cm^{-1} and pyranose ring. The insertion of TiO_2-NPs in the *B* method affects several chemical bond structures in CA and PEG organic materials. Whereas in both membranes, namely CA/PEG/TiO_2 *SC* and *B* methods, it provides good wave number absorption at 372 $cm^{-1,}$ showing the presence of O-Ti-O bonds formed due to the addition of TiO_2 material.

The CA and PEG form long-chain aliphatic bonds to form strong polymers, allowing CA membranes to have good hydrophilicity [31]. CA/PEG-based membrane where water tends to diffuse as a single molecule rather than groups or aggregates, the effectiveness of the filtration process goes well. Adding TiO_2 to the CA/PEG membrane lattice provides chemical

strength and functions as a photocatalyst material. PEG can increase gas permeability because the flexible PEG main chain allows the penetrant to diffuse easily through the membrane composite.

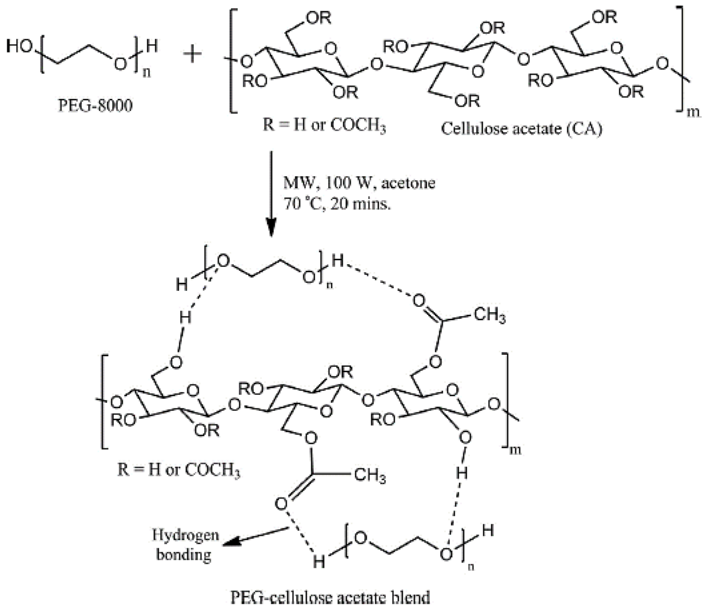

Figure 5. Chemical bonds of PEG and CA form the membrane polymer.

Figure 5 shows the CA and PEG membrane formation model simulated by [32], which shows that when PEG is dissolved in acetone and cellulose acetate is added, several bonds are present, such as -OH bonds derived from hydrogen bonds, aromatic rings (C-H), alkenes (C=H), and C-O-C. The presence of TiO_2 in the CA/PEG membrane influences the membrane structure, as done by [33], where the membrane is inserted with calcium oxide, forming intermolecular and intramolecular bonds (Figure 6).

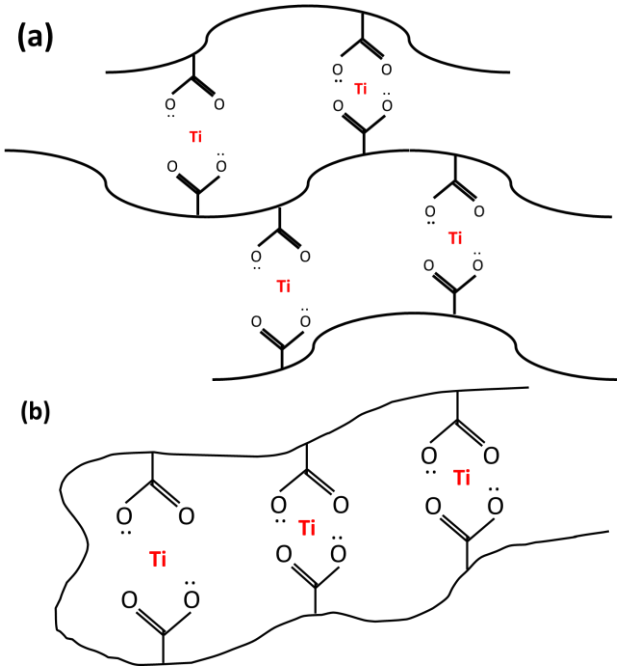

Figure 6. Formation probability of TiO_2-NPs with CA/PEG membrane; **(a)** intermolecular, and **(b)** intramolecular.

3.2.3. Scanning Electron Microscopy (SEM)

Surface morphology testing and a side view of the membrane were applied against CA/PEG, CA/PEG/TiO_2 *SC*, and *B* provide different surface morphology. Based on the surface morphology analysis (Figure 7a), the CA/PEG control membrane gave a smooth morphology and slightly formed pores. This density showed that the CA/PEG bond influenced the smooth structure and small pore density, as shown by the side view morphological characterization (Figure 7d). The mixture of PEG and CA showed a network structure at low magnification for all compositions with an even distribution of both phases. Thus, PEG is well dispersed on cellulose. The smooth effect on the surface of the CA/PEG membrane resulted from the effect of PEG addition. While the effect of TiO_2 with *SC* method (Figure 7b) shows the appearance of pores that are numerous and regular.

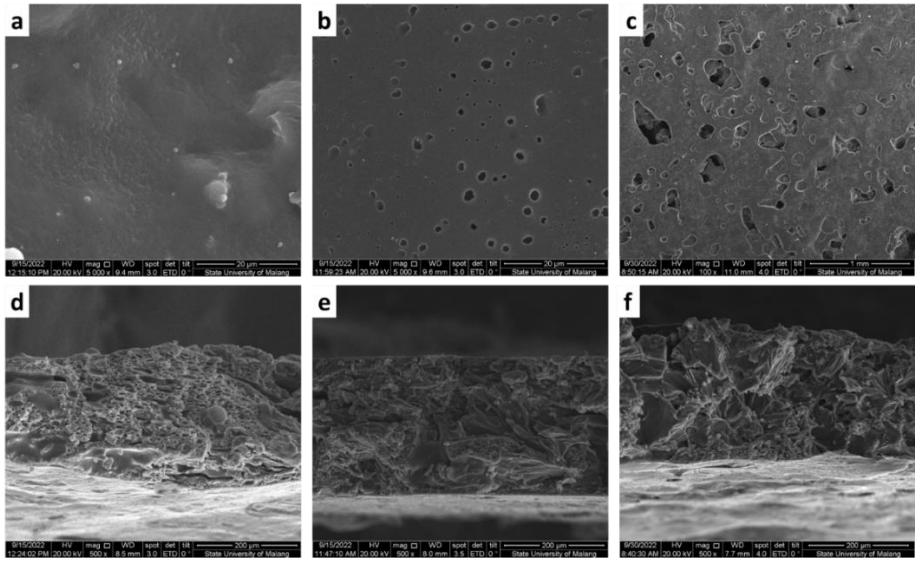

Figure 7. Surface morphology, (**(a)** CA/PEG, **(b)** CA/PEG/TiO_2 *SC*, and **(c)** CA/PEG/TiO_2 *B*); Side view morphology, (**(d)** CA/PEG, **(e)** CA/PEG/TiO_2 *SC*, and **(f)** CA/PEG/TiO_2 *B*).

The SC method only affects the surface of the membrane so that it does not affect the structural level of the side view (Figure 7e). Figure 6c is the surface morphology of the B method showing TiO_2-NPs inserted in the CA/PEG membrane pore lattice, and this is evidenced in the morphology of the side view of the CA/PEG/TiO_2 B (Figure 7f) that white grains are visible in each membrane pore lattice. Based on research by Kim *et al*. showed that the CA/PEG structure forms hollow fibers or structures following the sponge model where the middle of the membrane forms hollow fibers. This model relates to water being a strong non-solvent absorbed in the membrane lattice.

In addition, the effect of TiO_2 granules affects the formation of membrane pores. This model gives the effect that the membrane formed a semi-crystalline crystalline model. Where the crystalline model is indicated by the presence of TiO_2, while the amorphous structure of the effect given by cellulose acetate of the membrane made [32]. The morphological change of cellulose acetate increases the crystallization ability of PEG and reduces the resistance with increasing PEG concentration. In addition, the role of hydrogen bonding in the membrane also affects the material's crystallinity. Hydrogen bonds are further reduced when the presence of PEG dissolves in organic solvents. Then, quickly, hydrogen bonds from either water or solvent will easily evaporate and cool down, creating high crystallinity [34].

3.3. Reverse Osmosis (RO) Filtration

This research developed a simple RO-based filtration device to test the feasibility of the membrane's role in desalinating seawater. The designed tool is shown in Figure 8. Based on Figure 8, it can be seen that the filtration device is made of a 2-inch diameter PVC pipe, which is then divided into 3 tubes (compartments), each of which has a function. First, tube 1 stores feed (sample) water pre-treated with activated charcoal. Next, the water enters the 2nd tube system containing sand, stone, charcoal, and palm fiber for seawater filtration. This function also reduces seawater hardness levels and some impurities in the water. According to Sudrajat *et al*., this combination of filter materials allows the absorption of pollutants contained in water, such as odor, color, small particles, and other chemicals.

This tool is used where water enters the 1.5-liter tube 1 compartment and flows into tube 2 with a pump to enter the water in the initial filtering process. Sand in tube 2 serves to remove mud, soil, and small particles [35]. Stone and charcoal channel coarse particles in the water and charcoal channels or remove odors and toxins in water and clean water [36]. Furthermore, tube 3 consists of synthesized membranes, namely CA/PEG, CA/PEG/TiO_2 SC, and CA/PEG/TiO_2 B, which are tested alternately to see the optimization of the seawater desalination process. Tube 3 is also equipped with a UV lamp that activates the performance of TiO2 material to increase the ability to photodegrade harmful organic compounds. On the other hand, UV lamps also reduce the bacterial content in water samples so that water is free of microorganisms. The final result obtained by the filtered water can be harvested through the outlet channel.

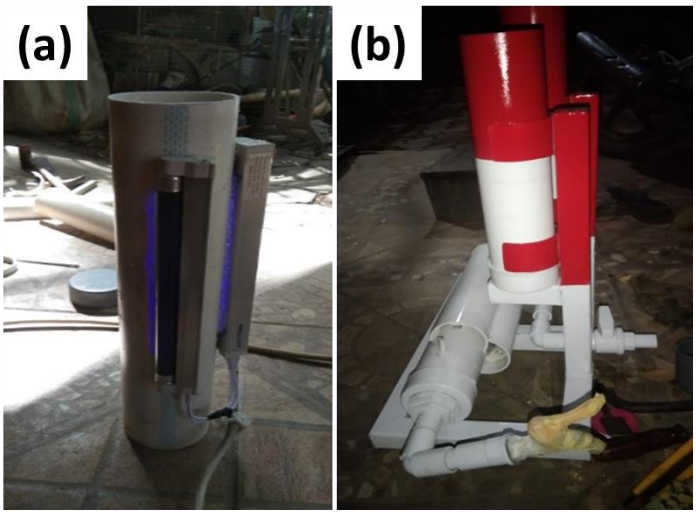

Figure 8. Design of a simple RO-based seawater desalination device.

3.4. Membrane performance test.

3.4.1. Water Flux Identification.

Flux value is the amount of permeate volume that passes through the membrane in one unit surface area of the membrane made under certain time conditions and supported by the pressure force of the RO water filtration system. Some factors that affect the flux value are membrane composition (membrane type) and the pressure applied. Flux testing on the membrane to see the rate of permeate velocity when the filtration process takes place. This is also influenced by the membrane pores. The larger the membrane pores, the more water molecules are missed; this is also the better the membrane permeability value, or the higher the

water flux value, the better the membrane permeability value. Factors that affect flux flow include membrane composition and pressure. The greater the pressure, the greater the flux produced. The pressure used in this study is constant at 10 bar. The driving force exerted causes pressure on seawater molecules so that the volume of brackish water passing through the membrane per unit area per unit time increases [37].

Based on the experimental results, it shows that the value of the volume of water produced has different variations from each membrane. This can be seen in Table 2 and Figure 9. Based on the CA/PEG membrane, the volume produced is 0.19 liters with a flux value of 98.80 L/m^2.h. These results explain that the CA/PEG membrane has a small porosity, so the water passing through the membrane is less than the two membranes modified with TiO_2 material. The TiO_2-modified CA/PEG membrane with *SC* method increased in flux value of 130 L/m^2.h, and the membrane with *B* method has a large value compared to the two membranes, which is 161.20 L/m^2.h. The greater the flux value, the greater the permeability value. The greater the flux value, the better the permeability value because the amount of permeate passed in a certain time is greater. The size of the pores in CA/PEG/TiO_2 *B* affects the seawater desalination process because the addition of TiO_2 gives the effect of strength and increases the filtering process so that salt components can be absorbed in the pore lattice of the membrane with the *B* method. TiO_2 has a role in inactivating microorganisms in water, increasing hydrophilic properties, and overcoming harmful organic matter. Therefore, the simultaneous addition of TiO_2 material can play an important role in simultaneously increasing the hydrophilicity and porosity of the membrane.

Table 2. The result of identifying the calculation value of membrane flux value.

Treatments	*Q* (Liter)	*d* (diameter) (m)	*r* (radius) (m)	r^2 (m^2)	*π*	*A*	*t* (hour)
CA/PEG (Control)	0.19	0.07	0.035	12.25×10^{-4}	3.14	38.465×10^{-4}	0.5
CA/PEG/TiO_2 (*SC*)	0.25	0.07	0.035	12.25×10^{-4}	3.14	38.465×10^{-4}	0.5
CA/PEG/TiO_2 (*B*)	0.31	0.07	0.035	12.25×10^{-4}	3.14	38.465×10^{-4}	0.5

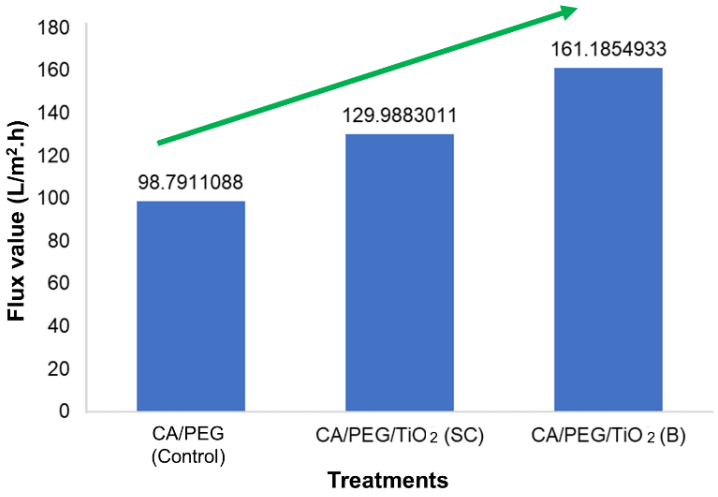

Figure 9. Calculation of flux values of each membrane

3.4.2. Salt rejection.

The synthesized membrane was then tested for its ability to salt rejection. The salt rejection calculation aims to observe the membrane's ability to hold, filter, and or pass certain organic substances contained in seawater. This determination of salt rejection can be expressed

as the selectivity of a membrane where a membrane with good ability can reject salt well or retain inorganic/organic components in seawater. Several factors can affect the membrane's salt rejection performance, such as dissolved particles, membrane pore size, and the size of particles passing through the membrane. Table 3 is the result of the salt rejection analysis of each membrane.

Table 3. Calculation of salt rejection value from membrane testing.

Treatments	**C_p (Permeate concentration; ‰)**	**C_0 (Seawater concentration; ‰)**	***Salt rejection* (%)**
Pretreatment	25	32	22%
CA/PEG (Control)	10	25	60%
CA/PEG/TiO_2 (*SC*)	5	25	80%
CA/PEG/TiO_2 (*B*)	4	25	84%

Based on Table 3, it can be seen that the identification of salt rejection from each membrane is different. The filtering material consisting of sand, stone, charcoal, and palm fiber has the ability to filter salt from seawater from 32‰ to 25‰. It can be assumed that the filtering material can reject salt by 7‰. When the CA/PEG membrane is added as a control, it can be affected by 60%, where the C_0 value of 25‰ is the result of the permeate concentration passing through the filtering material. Likewise, the CA/PEG/TiO_2 *SC* and *B* membranes have a salt rejection value of 80% and 84%, respectively. The higher the salt rejection, the better the membrane can hold, filter, and pass certain organic substances contained in seawater. The role of TiO_2-NPs combined with CA/PEG functions in retaining the salt contained in seawater has a function to reduce salinity because the presence of TiO_2-NPs activates the membrane pores, which have a dual function as a barrier/filter and absorber.

3.4.3. pH test.

Determination of the initial pH value of the seawater was examined to see the decrease in pH before and after the filtration process. The pH analysis of the seawater was initially identified to see the effect of the decrease in pH due to the filtration process. Based on Figure 9, it can be seen that the filtration process using the filtering material experienced a good decrease in pH to 8, while the role of CA/PEG, CA/PEG/TiO_2 *SC*, and *B* membranes experienced a decrease in pH of 7.9, 7.8, and 7.8.

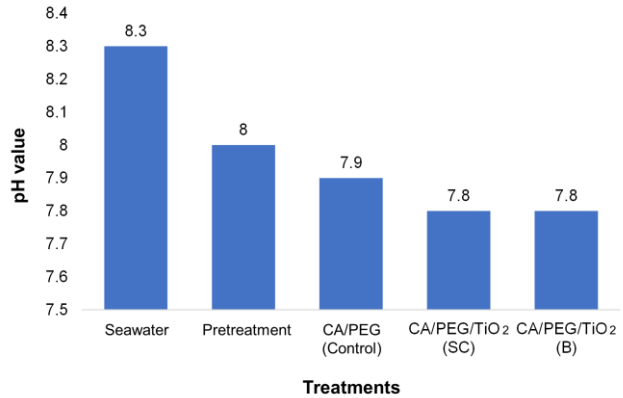

Figure 10. Results of pH determination of seawater desalination process.

Filter materials positively reduce pH because the role of sand, stone, charcoal, and fiber provides a good variation in acid-base conditions. Sand influences acidity due to the presence

of SiO_2 forming monosilicic acid $Si(OH)_4$ [38]. In addition, other inorganic elements in the sand, such as Al_2O_3, meet with NaOH from seawater to form acid [39]. Figure 9 shows a decrease of 0.3; 0.1; 0.2, and 0.2, respectively. TiO_2-NPs have a good effect in reducing pH, although not too significant with filter material. TiO_2 has the ability as a weakly acidic inorganic metal consisting of one or more inorganic compounds to form hydrogen ions and conjugated base ions when dissolved in water [40,41].

3.4.4. Salinity test.

One of the physical parameters that can be used as a water quality parameter is salinity or salt content. Salinity is determined using a refractometer. The salt content of seawater is the weight in grams of all solids dissolved in 1 kg of seawater; if all inorganic ions (bromine and iodine) are replaced with an equivalent amount of chlorine, all carbonates are converted to their oxides and all organic substances are oxidized. The measurement of salt content is related to chlorinity. This chlorinity includes chloride, bromide, and iodide. High and low salinity are influenced by several factors, namely temperature, evaporation, rainfall, and the number of rivers that empty into the sea, which affect the concentration of solutes and solvents. The higher the solution concentration, the higher the absorbency of the salt to absorb water. The salt content can be determined using a conductometer, salinity meter, turbidity meter, or electrode sensor.

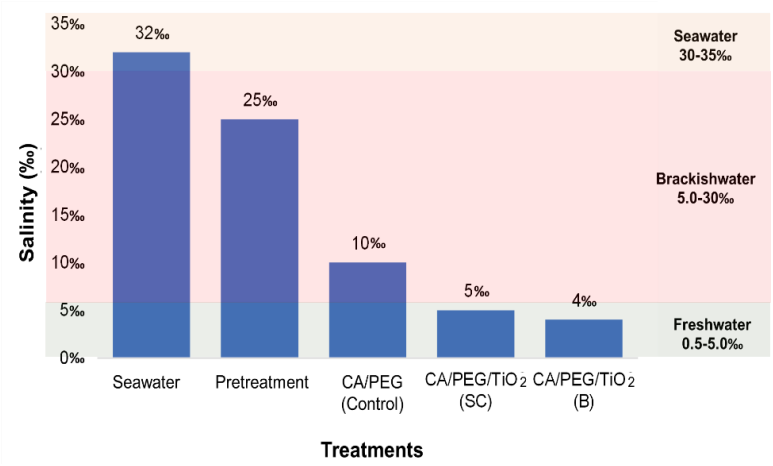

Figure 11. Results of salinity content under seawater desalination process.

Table 4. Classification of water salinity based on several researchers.

Classification of Seawater Salinity by [42]		**Groundwater Classification Based on Salinity by** [43]	
Salinity index (‰)	**Salinity Type**	**Salinity index (‰)**	**Salinity Type**
0.5-5.0	**Freshwater**	**Freshwater**	
		< 0,5	*Freshwater*
		0,5 – 3,0	*Oligohaline*
5.0-30	**Brackishwater**	**Brackishwater**	
		3,0 – 16	*Mesohaline*
		16 – 30	*Polyhaline*
30-35	**Seawater**	**Seawater**	
		30 – 40	*Marine*

Based on the identification of salinity contents (Figure 11) that have been passed through the filtering process (desalination) shows a decrease in seawater salt content respectively by 25‰ filter material, 10‰ CA/PEG membrane control, 5‰ CA/PEG/TiO_2 SC,

and 4‰ CA/PEG/TiO_2 B. This decrease, when compared to the classification of seawater salinity (Table 4), shows that the water that has been treated using CA/PEG/TiO_2 SC and B membranes was categorized as freshwater. When referring to research, this result is that the filtered water is categorized as brackish water with mesohaline salinity type, which is water that falls into the surface water category that still has mineral content.

4. Conclusions

CA/PEG membrane modified with TiO_2-NPs has been synthesized through SC and B methods. The results show that the B method performs well in desalinating seawater. The results are shown in the form of semi-crystalline with good porosity in filtering seawater with the value of water flux and salt rejection, which has a good value in holding the salt content in seawater. Design of seawater treatment equipment reverse osmosis system into clean water using CA/PEG/TiO_2 membrane B method provides a good ability to reduce salt content in seawater. The processing system is based on 3 compartments, namely seawater storage tubes, filter material tubes, and TiO_2-modified CA/PEG membrane tubes, with the addition of UV light. The role of TiO_2 has a significant effect on permeate water quality.

Funding

We acknowledge the financial support from the Ministry of Education, Culture, Research and Technology of the Republic of Indonesia under the basic research award grant no. 51/UN29.20/PG/2022 and the World Class Professor Award grant no. 3252/E4/DT.04.03/2022.

Acknowledgments

The authors would like to thank the Environmental Engineering Laboratory of Universitas Muhammadiyah Kendari for facilitating this research.

Conflicts of Interest

The authors declare that they have no known competing financial interests or personal relationships that could have appeared to influence the work reported in this paper.

References

1. Re, V.; Rizzi, J.; Tuci, C.; Tringali, C.; Mancin, M.; Mendieta, E.; Marcomini, A. Challenges and Opportunities of Water Quality Monitoring and Multi-Stakeholder Management in Small Islands: The Case of Santa Cruz, Galápagos (Ecuador). *Environ. Dev. Sustain.* **2022**, 1–25,, https://link.springer.com/article/10.1007/s10668-022-02219-4.
2. Sembiring, H.; A. Subekti, N.; Nugraha, D.; Priatmojo, B.; Stuart, A.M. Yield Gap Management under Seawater Intrusion Areas of Indonesia to Improve Rice Productivity and Resilience to Climate Change. *Agriculture* **2019**, *10*, 1, https://doi.org/10.3390/agriculture10010001.
3. Li, J.; Sun, J.; Li, Z.; Meng, X. Recent Advances in Electrocatalysts for Seawater Splitting in Hydrogen Evolution Reaction. *Int. J. Hydrogen Energy* **2022**, *47*, 29685-29697, https://doi.org/10.1016/j.ijhydene.2022.06.288.
4. Nugroho, H.Y.S.H.; Indrawati, D.R.; Wahyuningrum, N.; Adi, R.N.; Supangat, A.B.; Indrajaya, Y.; Putra, P.B.; Cahyono, S.A.; Nugroho, A.W.; Basuki, T.M. Toward Water, Energy, and Food Security in Rural Indonesia: A Review. *Water* **2022**, *14*, 1645, https://doi.org/10.3390/w14101645.
5. Lebel, L.; Navy, H.; Siharath, P.; Long, C.T.M.; Aung, N.; Lebel, P.; Hoanh, C.T.; Lebel, B. COVID-19 and Household Water Insecurities in Vulnerable Communities in the Mekong Region. *Environ. Dev. Sustain.*

2022, 1–20, https://link.springer.com/article/10.1007/s10668-022-02182-0.
6. Nthunya, L.N.; Bopape, M.F.; Mahlangu, O.T.; Mamba, B.B.; Van der Bruggen, B.; Quist-Jensen, C.A.; Richards, H. Fouling, Performance and Cost Analysis of Membrane-Based Water Desalination Technologies: A Critical Review. *J. Environ. Manage.* **2022**, *301*, 113922, https://doi.org/10.1016/j.jenvman.2021.113922.
7. Nagar, A.; Pradeep, T. Clean Water through Nanotechnology: Needs, Gaps, and Fulfillment. *ACS Nano* **2020**, *14*, 6420–6435, https://pubs.acs.org/doi/10.1021/acsnano.9b01730.
8. Binger, Z.M.; Achilli, A. Forward Osmosis and Pressure Retarded Osmosis Process Modeling for Integration with Seawater Reverse Osmosis Desalination. *Desalination* **2020**, *491*, 114583, https://doi.org/10.1016/j.desal.2020.114583.
9. Kingsbury, R.S.; Wang, J.; Coronell, O. Comparison of Water and Salt Transport Properties of Ion Exchange, Reverse Osmosis, and Nanofiltration Membranes for Desalination and Energy Applications. *J. Memb. Sci.* **2020**, *604*, 117998, https://doi.org/10.1016/j.memsci.2020.117998.
10. Li, Y.; Yang, S.; Zhang, K.; Van der Bruggen, B. Thin Film Nanocomposite Reverse Osmosis Membrane Modified by Two Dimensional Laminar MoS2 with Improved Desalination Performance and Fouling-Resistant Characteristics. *Desalination* **2019**, *454*, 48–58, https://doi.org/10.1016/j.desal.2018.12.016.
11. Boussouga, Y.-A.; Richards, B.S.; Schäfer, A.I. Renewable Energy Powered Membrane Technology: System Resilience under Solar Irradiance Fluctuations during the Treatment of Fluoride-Rich Natural Waters by Different Nanofiltration/Reverse Osmosis Membranes. *J. Memb. Sci.* **2021**, *617*, 118452, https://doi.org/10.1016/j.memsci.2020.118452.
12. Castro-Muñoz, R. Breakthroughs on Tailoring Pervaporation Membranes for Water Desalination: A Review. *Water Res.* **2020**, *187*, 116428, https://doi.org/10.1016/j.watres.2020.116428.
13. Zahid, M.; Rashid, A.; Akram, S.; Rehan, Z.A.; Razzaq, W. A Comprehensive Review on Polymeric Nano-Composite Membranes for Water Treatment. *J. Membr. Sci. Technol* **2018**, *8*, 1–20, https://www.walshmedicalmedia.com/open-access/a-comprehensive-review-on-polymeric-nanocomposite-membranes-for-water-treatment-2155-9589-1000179.pdf.
14. Zhang, J.; Wang, Z.; Wang, Q.; Pan, C.; Wu, Z. Comparison of Antifouling Behaviours of Modified PVDF Membranes by TiO2 Sols with Different Nanoparticle Size: Implications of Casting Solution Stability. *J. Memb. Sci.* **2017**, *525*, 378–386, https://doi.org/10.1016/j.memsci.2016.12.021.
15. Etemadi, H.; Fonouni, M.; Yegani, R. Investigation of Antifouling Properties of Polypropylene/TiO2 Nanocomposite Membrane under Different Aeration Rate in Membrane Bioreactor System. *Biotechnol. reports* **2020**, *25*, e00414, https://doi.org/10.1016/j.btre.2019.e00414.
16. Ahmad, A.; Waheed, S.; Khan, S.M.; Shafiq, M.; Farooq, M.; Sanaullah, K.; Jamil, T. Effect of Silica on the Properties of Cellulose Acetate/Polyethylene Glycol Membranes for Reverse Osmosis. *Desalination* **2015**, *355*, 1–10, https://doi.org/10.1016/j.desal.2014.10.004.
17. Goetz, L.A.; Jalvo, B.; Rosal, R.; Mathew, A.P. Superhydrophilic Antifouling Electrospun Cellulose Acetate Membranes Coated with Chitin Nanocrystals for Water Filtration. *J. Memb. Sci.* **2016**, *510*, 238–248, https://doi.org/10.1016/j.memsci.2016.02.069.
18. Kheilnezhad, B.; Hadjizadeh, A. Ibuprofen-Loaded Electrospun PCL/PEG Nanofibrous Membranes for Preventing Postoperative Abdominal Adhesion. *ACS Appl. Bio Mater.* **2022**, *5*, 1766–1778, https://doi.org/10.1021/acsabm.2c00126.
19. Feng, D.; Feng, Y.; Li, P.; Zang, Y.; Wang, C.; Zhang, X. Modified Mesoporous Silica Filled with PEG as a Shape-Stabilized Phase Change Materials for Improved Thermal Energy Storage Performance. *Microporous Mesoporous Mater.* **2020**, *292*, 109756, https://doi.org/10.1016/j.micromeso.2019.109756.
20. Ali, M.; Jahan, Z.; Sher, F.; Niazi, M.B.K.; Kakar, S.J.; Gul, S. Nano Architectured Cues as Sustainable Membranes for Ultrafiltration in Blood Hemodialysis. *Mater. Sci. Eng. C* **2021**, *128*, 112260, https://doi.org/10.1016/j.msec.2021.112260.
21. Ounifi, I.; Guesmi, Y.; Ursino, C.; Castro-Muñoz, R.; Agougui, H.; Jabli, M.; Hafiane, A.; Figoli, A.; Ferjani, E. Synthesis and Characterization of a Thin-Film Composite Nanofiltration Membrane Based on Polyamide-Cellulose Acetate: Application for Water Purification. *J. Polym. Environ.* **2022**, *30*, 707–718, https://link.springer.com/article/10.1007/s10924-021-02233-z.
22. Li, J.-H.; Yan, B.-F.; Shao, X.-S.; Wang, S.-S.; Tian, H.-Y.; Zhang, Q.-Q. Influence of Ag/TiO2 Nanoparticle on the Surface Hydrophilicity and Visible-Light Response Activity of Polyvinylidene Fluoride Membrane. *Appl. Surf. Sci.* **2015**, *324*, 82–89, https://doi.org/10.1016/j.apsusc.2014.10.080.
23. Hikmawati; Watoni, A.H.; Wibowo, D.; Maulidiyah; Nurdin, M. Synthesis of Nano-Ilmenite (FeTiO3)

Doped TiO2/Ti Electrode for Photoelectrocatalytic System. *IOP Conf. Ser. Mater. Sci. Eng.* **2017**, *267*, 012005, https://doi.org/10.1088/1757-899X/267/1/012005.
24. Natsir, M.; Putri, Y.I.; Wibowo, D.; Maulidiyah, M.; Salim, L.O.A.; Azis, T.; Bijang, C.M.; Mustapa, F.; Irwan, I.; Arham, Z. Effects of Ni–TiO2 Pillared Clay–Montmorillonite Composites for Photocatalytic Enhancement against Reactive Orange under Visible Light. *J. Inorg. Organomet. Polym. Mater.* **2021**, *31*, 3378–3388, https://link.springer.com/article/10.1007/s10904-021-01980-9.
25. Agboola, O. The Role of Membrane Technology in Acid Mine Water Treatment: A Review. *Korean J. Chem. Eng.* **2019**, *36*, 1389–1400, https://link.springer.com/article/10.1007/s11814-019-0302-2.
26. Bodzek, M.; Konieczny, K.; Kwiecińska, A. Application of Membrane Processes in Drinking Water Treatment–state of Art. *Desalin. Water Treat.* **2011**, *35*, 164–184, https://doi.org/10.5004/dwt.2011.2435.
27. Chu, L.; Qin, Z.; Yang, J.; Li, X. Anatase TiO2 Nanoparticles with Exposed {001} Facets for Efficient Dye-Sensitized Solar Cells. *Sci. Rep.* **2015**, *5*, 1–10, https://www.nature.com/articles/srep12143.
28. El-Desoky, M.M.; Morad, I.; Wasfy, M.H.; Mansour, A.F. Synthesis, Structural and Electrical Properties of PVA/TiO2 Nanocomposite Films with Different TiO2 Phases Prepared by Sol–gel Technique. *J. Mater. Sci. Mater. Electron.* **2020**, *31*, 17574–17584, https://link.springer.com/article/10.1007/s10854-020-04313-7.
29. Wang, J.; Yu, J.; Zhu, X.; Kong, X.Z. Preparation of Hollow TiO 2 Nanoparticles through TiO 2 Deposition on Polystyrene Latex Particles and Characterizations of Their Structure and Photocatalytic Activity. *Nanoscale Res. Lett.* **2012**, *7*, 1–8, https://link.springer.com/article/10.1186/1556-276X-7-646.
30. Mofokeng, L.E.; Hlekelele, L.; Moma, J.; Tetana, Z.N.; Chauke, V.P. Energy-Efficient CuO/TiO2@ GCN Cellulose Acetate-Based Membrane for Concurrent Filtration and Photodegradation of Ketoprofen in Drinking and Groundwater. *Appl. Sci.* **2022**, *12*, 1649, https://doi.org/10.3390/app12031649.
31. Kim, K.; Ingole, P.G.; Yun, S.; Choi, W.; Kim, J.; Lee, H. Water Vapor Removal Using CA/PEG Blending Materials Coated Hollow Fiber Membrane. *J. Chem. Technol. Biotechnol.* **2015**, *90*, 1117–1123, https://doi.org/10.1002/jctb.4421.
32. Sundararajan, S.; Samui, A.B.; Kulkarni, P.S. Shape-Stabilized Poly (Ethylene Glycol)(PEG)-Cellulose Acetate Blend Preparation with Superior PEG Loading via Microwave-Assisted Blending. *Sol. Energy* **2017**, *144*, 32–39, https://doi.org/10.1016/j.solener.2016.12.056.
33. Siva, T.; Muralidharan, S.; Sathiyanarayanan, S.; Manikandan, E.; Jayachandran, M. Enhanced Polymer Induced Precipitation of Polymorphous in Calcium Carbonate: Calcite Aragonite Vaterite Phases. *J. Inorg. Organomet. Polym. Mater.* **2017**, *27*, 770–778, https://link.springer.com/article/10.1007/s10904-017-0520-1.
34. Liu, T.; Lu, H.; Li, C.; Chen, L.; Feng, Z. Excellent Effect of Lubrication Performance of Chitosan/Polyethylene Glycol/Palygorskite as Water-based Lubricating Additive on 304 Stainless Steel and Polymer Pairs. *Polym. Eng. Sci.* **2022**, https://doi.org/10.1002/pen.25980.
35. Sikiru, S.; Ayodele, O.J.A.; Sanusi, Y.K.; Adebukola, S.Y.; Soleimani, H.; Yekeen, N.; Haslija, A.B.A. A Comprehensive Review on Nanotechnology Application in Wastewater Treatment a Case Study of Metal-Based Using Green Synthesis. *J. Environ. Chem. Eng.* **2022**, 108065, https://doi.org/10.1016/j.jece.2022.108065.
36. Yazidi, A. Rancangan Alat Filtrasi Pada Sistem Pengolahan Air Bersih Kapasitas 7, 5 Liter **2021**, http://eprints.uniska-bjm.ac.id/9163/.
37. Xie, R.; Ning, P.; Qu, G.; Li, J.; Ren, M.; Du, C.; Gao, H.; Li, Z. Self-Made Anion-Exchange Membrane with Polyaniline as an Additive for Sulfuric Acid Enrichment. *Chem. Eng. J.* **2018**, *341*, 298–307, https://doi.org/10.1016/j.cej.2018.02.012.
38. Gu, Y.; Wang, L.; Chen, J.; Jiang, Z.; Zhang, Y.; Wang, W.; Chen, H.; Shen, J.; Zhong, J.; Meng, S. Surface Acidity of Colloidal Silica and Its Correlation with Sapphire Surface Polishing. *Colloids Surfaces A Physicochem. Eng. Asp.* **2022**, *651*, 129718, https://doi.org/10.1016/j.colsurfa.2022.129718.
39. Joseph, C.G.; Yap, Y.H.T.; Krishnan, V.; Puma, G.L. Application of Modified Red Mud in Environmentally-Benign Applications: A Review. **2019**, https://www.researchgate.net/publication/337426049_Application_of_modified_red_mud_in_environmentally-benign_applications_A_review_paper.
40. Speight, J.G. *Reaction Mechanisms in Environmental Engineering: Analysis and Prediction*; Butterworth-Heinemann, 2018; ISBN 0128006676, https://www.sciencedirect.com/book/9780128044223/reaction-mechanisms-in-environmental-engineering.
41. Speight, J.G. Industrial Inorganic Chemistry. *Environ. Inorg. Chem. Eng.* **2017**, *1*, https://shop.elsevier.com/books/environmental-inorganic-chemistry-for-engineers/speight/978-0-12-

849891-0.
42. Nybakken, J.W. Biologi Laut. *Suatu Pendekatan Ekol. PT Gramedia. Jakarta* **1992**, 325–363, https://lib.ui.ac.id/detail?id=140750.
43. Purnomo, A.S.; Rizqi, H.D.; Harmelia, L.; Anggraeni, S.D.; Melati, R.E.; Damayanti, Z.H.; Shafwah, O.M.; Kusuma, F.C. Biodegradation of Crude Oil by Ralstonia Pickettii under High Salinity Medium. *Malays. J. Fundam. Appl. Sci* **2019**, *15*, 377–380, https://mjfas.utm.my/index.php/mjfas/article/view/1181.